Role of the polyphenol content on the structuring behavior of liposoluble gelators in extra virgin olive oil

Francesco Ciuffarin [a], Marilisa Alongi [a,*], Donatella Peressini [a], Luisa Barba [b], Paolo Lucci [a], Sonia Calligaris [a]

[a] Department of Agricultural, Food, Environmental and Animal Sciences, University of Udine, 33100 Udine, Italy
[b] Institute of Crystallography, National Council of Research, 34100 Trieste, Italy

A R T I C L E   I N F O

A B S T R A C T

The role of polyphenols in affecting the structural and rheological properties of oleogels was investigated. Polyphenols were selectively removed from extra virgin olive oil (EVOO), and the resulting oils at three different polyphenol levels were gelled by using 10% (w/w) of monoglycerides (MG), rice wax (RW), sunflower wax (SW), and a mixture of β-sitosterol/γ-oryzanol (PS). The structural characteristics of oleogels were assessed by visual appearance, rheology, polarized light microscopy, calorimetry, XRD, and FTIR. Polyphenol content differently affected oleogel characteristics depending on network features. While EVOO-polyphenols did not influence PS- and SW-based oleogels, they reinforced MG- and RW-based oleogel network. As polyphenol content increased, the critical stress and melting temperature also increased, concomitantly with changes in crystal morphology. This was attributed to the capacity of polyphenols to form additional junction points in the crystalline network.

1. Introduction

Today, fat-containing foods - rich in saturated and trans fatty acids - are in the spotlight being their excessive intake worldwide recognized as closely associated with the risk of developing non-communicable diseases (*e.g.,* hypercholesterolemia, coronary heart disease, stroke, type II diabetes, obesity, and metabolic syndrome) (Hooper et al., 2020). Additionally, the use of fats brings about environmental sustainability issues, as in the case of palm and other tropical oils (Vijay, Pimm, Jenkins, & Smith, 2016). Thus, technological strategies enabling the production of more sustainable fat sources, both from nutritional and environmental viewpoints, are highly demanded. These strategies are in line with the "Farm to Fork Strategy" document released in 2020 by the EU Commission along with the EU Green Deal (Europena Commission, 2020) asking to boost the transition to more sustainable food consumption.

Extra virgin olive oil (EVOO), which is widely consumed within the Mediterranean diet, represents an excellent source of lipids, being characterized by an optimally balanced fatty acid profile and by the presence of minor components, such as polyphenols, with demonstrated health-promoting properties (Martín-Peláez et al., 2017; Owen et al., 2000). These positive nutritional features make EVOO an optimal candidate to design healthy foods, inspiring the boosting of its use in complex foods.

One of the most promising strategies to enlarge the applicability of EVOO is its conversion into a gel-like material, named oleogel, with functionalities comparable to those of plastic fats (Marangoni & Garti, 2018). By definition, an oleogel is a gel in which a continuous liquid oil phase is immobilized into a supramolecular network of self-assembled molecules known as oleogelators (Co & Marangoni, 2012; Patel & Dewettinck, 2016). Until now, several gelators have been studied and proposed, such as low molecular lipophilic components and polymeric substances (Patel & Dewettinck, 2016). The gelation is generally obtained by direct or indirect methodologies. The first one implies the dissolution of one or more lipophilic gelators into liquid oil under proper physicochemical conditions. The resulting solution is then cooled to induce the gelator to self-assemble into a network entrapping oil (Patel & Dewettinck, 2016). On the other hand, indirect oleogelation is applied to obtain oleogels containing hydrophilic biopolymers, such as proteins and carbohydrates (Patel, 2020).

It was previously demonstrated the possibility to gel EVOO by different oleogelators mainly by the direct method (Alongi, Lucci, Clodoveo, Schena, & Calligaris, 2022; Calligaris, Mirolo, da Pieve, Arrighetti, & Nicoli, 2014; Giacintucci et al., 2018; Valoppi, Calligaris, &

Marangoni, 2017; Yilmaz & Öłütcü, 2015). Nowadays, it has been also demonstrated that the structuring capacity of oleogelators cannot be decoupled from the features of the oil to be gelled. In particular, oil chemical characteristics, in terms of fatty acid profile and presence of minor components, are the main parameters affecting the final oleogel structure.

Up to now, no research effort has been dedicated to the effect of EVOO minor components on oleogel structure, excluding the case of ethylcellulose studied by Giacintucci et al. (2018). These authors highlighted the critical role of polyphenols in determining the structural and mechanical properties of the final gel network. It was demonstrated that as polyphenol content decreased, the gel network resulted more heterogeneous and disordered with irregular and elongated-shaped pores, and such a result was attributed to the surface activity of polyphenols.

Based on these considerations, the aim of this work was to investigate the role of polyphenols on the structural and rheological properties of EVOO-based oleogels prepared by exploiting the gelling ability of well-known gelators, *i.e.*, saturated monoglycerides, rice wax, sunflower wax, or a mixture of γ-oryzanol and β-sitosterol. These gelators were selected based on their well-known ability to gel plant-based oils (Co & Marangoni, 2012; Martins, Vicente, Cunha, & Cerqueira, 2018), including EVOO (Alongi et al., 2022). It should be said that the resulting oleogels are characterized by the presence of differently structured networks. Monoglycerides and waxes form crystalline tridimensional networks in oil (da Pieve, Calligaris, Co, Nicoli, & Marangoni, 2010; Doan, van de Walle, Dewettinck, & Patel, 2015), whereas the mixture of γ-oryzanol and β-sitosterol assembles into a fibrillar network (Bot, den Adel, & Roijers, 2008). To unravel the effect of the presence of polyphenols on oleogel structure, polyphenols were selectively removed from the EVOO before gelation with 10% (w/w) of each gelator. This concentration was considered to be able to generate firm oleogels with high oil holding capacity (Alongi et al., 2022). The structural characteristics of oleogels were assessed by different methodologies, including rheology, polarized light microscopy, calorimetry, synchrotron XRD, and FTIR. Results clearly demonstrated the polyphenol structuring ability.

2. Materials and methods

2.1. Materials

Commercial extra virgin olive oil (EVOO) was used. Myverol™ saturated monoglycerides (fatty acid composition: 0.24% C12:0, 0.88% C14:0, 60.1% C16:0, 38.4% C18:0, 0.26% C20:0, 0.07% other; melting point 68.05 ± 0.5 °C) were purchased from Kerry Bioscience (Bristol, UK); rice bran wax (Karl Wax GmbH & Co. KG, Reinbek, Germany) was kindly provided by Spica Srl (Sulmona, Italy); sunflower wax purchased from Kahlwax GmbH & Co. KG (Reinbek, Germany), β-sitosterol (75.5% β-sitosterol, 12.0% β-sitostanol, 8.4% campesterol, 3.0% other) and γ-oryzanol (99% purity) were purchased from Nutraceutica S.r.l. (Monterenzio, Italy). Hydroxytyrosol, tyrosol, and tocopherol (α, γ, and δ-tocopherols) analytical standards, as well as all the other analytical grade reagents, were purchased from Sigma Aldrich (Milan, Italy).

2.2. Sample preparation

2.2.1. Polyphenol removal from EVOO

Polyphenols were removed from EVOO by using the official COI/T.20/Doc No 29 method. In particular, oil was mixed in a 2:5 (v/v) ratio with a methanol/water (80:20, v/v) solution, vortexed for 3 min, sonicated for 25 min, and centrifuged at 5,000 rpm for 15 min. The oil fraction was recovered and the same procedure was repeated 4 times. Afterward, the oil cleared from polyphenols (No-P) was mixed with the untreated oil (High-P) in a 1:1 ratio (v/v) to obtain a sample with an intermediated polyphenol content (Medium-P).

2.2.2. Oleogel preparation and storage

Oleogels were prepared by following the methodologies reported by Calligaris, Alongi, Lucci, and Anese (2020) and Alongi et al. (2022), with some modifications. In particular, 10% (w/w) of saturated monoglycerides (MG), rice wax (RW), sunflower wax (SW), or a mixture of β-sitosterol and γ-oryzanol (PS) (2:3, w/w), were added to the three oil samples having different polyphenol content. The mixtures were stirred in the dark at temperatures higher than the gelator melting point (i.e., 80 °C for MG, RW; SW, 90 °C for PS) until the complete melting of the gelator, which required about 20 min for MG, RW or SW, and 25 min for PS. The heating times were minimized to prevent polyphenols degradation as much as possible. Afterward, MG, RW, and SW oleogels were cooled and stored at room temperature (20 °C) in dark conditions, while PS oleogel was cooled at 4 °C for 12 h before being stored at 20 °C. All samples were analyzed 48 h after preparation to allow network setting.

2.3. Analytical determinations

2.3.1. Oil fatty acid composition

In order to determine fatty acid composition (%), the methyl-esters were prepared according to the COI/T.20 Doc No 33 method. Samples were methylated before injection in Thermo Trace (Thermo Fisher, Waltham, Massachusetts, USA) 1300 gas chromatograph equipped with a FID detector and an auto-sampler. A fused silica column, SP-2330 (60 m length × 0.32 mm i.d. × 0.20 μm film thickness), was used. Helium was employed as a carrier gas, with a flow through the column of 1 mL/min. The temperatures of the injector (split) and detector (FID) were both set at 250 °C. An injection volume of 1 μL was used. The operating conditions were as follows: oven temperature was held at 165 °C for 5 min, then increased by 3 °C min^{-1} to 210 °C and held for 10 min. The split ratio was 1:50. Results were expressed as a percentage of relative area.

2.3.2. Peroxide values

The peroxide number was determined based on the method COI/T.20/ Doc. No 35 Rev.1. Briefly, 5 g oil were weighed, added to 25 mL of isooctane/acetic acid (2:3, v/v) solution, and shaken for 5 min. An aliquot of 1 mL of freshly prepared potassium iodate saturated solution was added and the samples were shaken for another 1 min. Afterward, 25 mL water was added to stop the reaction, and 2 mL of a 10 g/L soluble-starch dispersion was added. Finally, samples were titrated with a 0.01 M sodium thiosulfate solution. The peroxide value (PV) was expressed as milliequivalents of active oxygen (mEqO$_2$) per kg of oil and computed by Eq. (1):

$$PV \; (mEqO_2/kg) = V \bullet M \bullet 1000 \tag{1}$$

where V is the volume of the sodium thiosulfate solution, M its concentration, and m the oil mass.

2.3.3. Absorbance at 232 and 270 nm

Absorbance was measured at 232 and 270 nm according to the method COI/T.20/Doc. No 19/Rev.5. Briefly, 0.25 g of sample was added with cyclohexane to 25 mL. Samples were properly diluted and absorbance at 232 and 270 nm was recorded (UV-2501PC, UV–VIS Recording Spectrophotometer, Shimadzu Corporation, Kyoto, Japan).

2.3.4. Diglycerides composition

Oil composition was analyzed using the method COI/T.20 Doc No 32 based on gas chromatography (GC Carlo Erba HRGC-5160, Milano, Italia). In particular, 0.1 g of oil was added with 1 mL of internal standard (dinonadecanoine in methyl-tertbutyl-ether, 0.1%). An aliquot of 30 μL of this solution was dried by a gentle nitrogen stream, added with 200 μL of silylation reagent and 200 μL of pyridine, mixed, left for 20 min to allow the complete reaction, and dried before adding 1 mL of *n*-heptane. Aliquots of 1 μL of the sample were injected (on column injection) at 80 °C eluted under helium pressure of 55 kPa. 80 °C have

been held for 1 min, then oven temperature increased from 80 to 340 °C in 41 min (2 min at 80 °C, 20 °C/min from 80 to 300 °C, 5 °C/min from 300 to 340 °C, and 20 min at 340 °C). A Mega SE52 (8 m long, 0.32 μm in diameter, 0.10 μm film thickness) column was used. Diglycerides were detected by a FID detector at 350 °C and quantified based on Eq. 2:

$$A\% = \frac{Ax \bullet ms}{As \bullet m} \bullet 100 \tag{2}$$

where *Ax* is the area corresponding to the peak of a single diglyceride, *As* is the area corresponding to the internal standard peak, *ms* is the added amount (mg) of internal standard, and *m* is the amount (mg) of the sample.

2.3.5. Hydroxytyrosol and tyrosol quantification

Hydroxytyrosol and tyrosol were extracted from 2 g of sample according to the official COI/T.20/Doc No 29 method. Acid hydrolysis was applied following the procedure suggested by Rovellini (2017). UHPLC analysis was performed using an Agilent Poroshell 120 EC-C18 reversed-phase column (2.7 μm particle size, 4.6 × 150 mm) on a Shimadzu Nexera UHPLC System (Shimadzu Nexera, Kioto, Japan) equipped with dual pump LC-30AD, on-line degasser DGU-20AS, column oven CTO-30A, autosampler SIL-30AC, and diode array detector (SPD-M20A) following the operative conditions described by Lucci, Bertoz, Pacetti, Moret, and Conte (2020). Polyphenol quantification was obtained through calibration curves in the range of 10–600 ng of tyrosol and hydroxytyrosol injected on-column with R^2 values higher than 0.999, in all cases. Polyphenol content in oil was calculated as the sum of hydroxytyrosol and tyrosol values.

2.3.6. Tocopherol quantification

Tocopherol was identified and quantified in accordance with the method reported by Lucci et al. (2020). Briefly, UHPLC analysis was realized using a Shimadzu Nexera (Shimadzu, Kyoto, Japan) coupled with the same components used for polyphenols analysis and a fluorescence detector RF-20Axs with double acquisition channels and a 12 μL cell. The detector was set at 296 nm and 325 nm for exciting and emission wavelengths, respectively. Oil samples were diluted in 2-propanol for reaching a 100 mg/mL concentration and 1 μL was injected on the column as a compromise between sensibility and column capacity. The chromatographic separation was performed using an Agilent Eclipse PAH column (1.8 μm particle size, 4.6 × 50 mm) used under isocratic conditions with solvent A (methanol) and B (acetonitrile) in the ratio 60/40 (v/v) and a total flow of 600 μL min^{-1}. The oven temperature was set to 30 °C. The injected volume for each sample was 1 μL. Tocopherols were quantified using a calibration curve for δ, β + γ, and α respectively in the range 0.05–100 ng injected on the column with R^2 values higher than 0.999.

2.3.7. Oil viscosity

Oil viscosity was measured using a rotational rheometer (Haake Rheostress 6000, Thermo Scientific, Karlsruhe, Germany), controlled through the Rheowin v.4.60.0001 software package (Thermo Scientific, Karlsruhe, Germany). Briefly, 20 mL oil was poured in a concentric cylinder geometry (CC25 DIN Ti) and rested for 5 min before testing. The flow behavior was determined at 20 °C from 0.3 to 100 s^{-1} of shear rate under steady state conditions (Haake UTM temperature controller unit, Thermo Scientific). Since a typical Newtonian behavior was observed, viscosity was a constant value defined as the ratio between shear stress and shear rate (Newton's law).

2.3.8. Wax fatty acids esters length

Crude rice wax and sunflower wax fatty acid compositions were obtained following the method of Wijarnprecha, Aryusuk, Santiwattana, Sonwai, and Rousseau (2018) with some modifications. An aliquot of 0.100 g of crude wax was dispersed in 4 mL of hexane, then 0.5 mL of the wax-containing solution was hydrolyzed with 2 N ethanolic KOH

(ethanol:water 80:20, v/v) for 8 h. The fatty acid ethyl esters (FAEE) analysis was performed on a Thermo-Trace 1300 (Thermo Scientific, Waltham, MA, USA) GC system, equipped with a flame ionization detector. Separation was carried out on an SP2330 (Supelco, Bellefonte, PA, USA) fused silica capillary column 30 m long, 0.25 mm ID, and 0.20 μm stationary phases film thickness. Samples of 1 μL were injected with a split ratio of 25:1. Helium was used as carrier gas at a flow rate of 1 mL min^{-1}. The injector and detector were stabilized at 250 °C, the column held at 170 °C for 2 min, then increased to 210 °C at a rate of 2 °C min^{-1} and maintained at 210 °C for 20 min.

2.4. Oleogel characterization

2.4.1. Macroscopic appearance

Gel images were acquired by using an image acquisition cabinet (Immagini and Computer, Bareggio, Italy) equipped with a digital camera (EOS 550D, Canon, Ota City, Tokyo, Japan) and 60 mm lens with 2.8 focal aperture (Canon, Ota City, Tokyo, Japan). The digital camera was placed on an adjustable stand positioned 40 cm in front of a black cardboard base where the sample was placed. The light was provided by four 23 W frosted photographic floodlights, in a position allowing minimum shadow and glare. Other camera settings were: shutter time 1/250 s, f/2.8, and focal length 60 mm. Images were saved in jpg format.

2.4.2. Polarized light microscopy

Samples were prepared by depositing a drop of a molten gel onto a heated glass microscope slide. The molten gel was pressed with a glass cover slip to ensure a sample thin enough for the measurement. Slides were allowed to cool at room temperature for 48 h before imaging at 20 °C. Images were taken at 40x and 400x magnification using a Leica EC3 digital camera, elaborated by the Leica Suite Las EZ software (Leica Microsystems, Heerbrugg, Switzerland) and saved in jpg format.

2.4.3. Oil binding capacity

The oil binding capacity (OBC) was determined by weighing about 1 g oleogel was allowed to be set directly into a microcentrifuge tube. Samples were centrifuged at 10,000 rpm for 15 min at 20 °C (Mikro 120, Hettich Zentrifugen, Andreas Hettich GmbH and Co, Tuttlingen, Germany) and decanted the excess oil. The samples were weighed and OBC was expressed as the percentage of oil retained by the oleogel.

2.4.4. Viscoelastic properties

The rheological properties of oleogels were determined using a controlled stress rheometer (Haake Rheostress 6000, Thermo Scientific, Karlsruhe, Germany). Aliquots of about 4 g of sample were gently transferred on a 35-mm parallel-plate geometry system, and the measuring gap and temperature were set at 2 mm and 20 °C, respectively. Due to the brittle texture of PS oleogel, samples were preliminarily prepared by carefully cutting, with a sharp knife, cylinders of 2-mm height and 35-mm diameter able to fit within the parallel-plate geometry gap to avoid gel breaking during loading. Samples were equilibrated for 5 min before testing to allow stress relaxation. Viscoelastic properties were evaluated using oscillatory stress sweep and frequency sweep tests. The former was performed to determine the upper limit of the linear viscoelastic region (LVR) and was carried out at 1 Hz and a stress amplitude in the range of 0.1–1000 Pa for MG, RW, or SW, and 100–5000 Pa for PS. The frequency sweep test was carried out at a constant stress amplitude selected within LVR, and a frequency range of 0.1–10 Hz. Storage modulus (G'), loss modulus (G''), and loss tangent (tan δ = G''/G') were measured. The critical stress (σ_c), where the G' value of the *plateau* reduces by 10% during the stress sweep test, was used as an index of oleogel resistance to shear stress (Doan et al., 2017). Viscoelastic parameters were compared at 1 Hz.

2.4.5. Thermal analysis

A TA4000 differential scanning calorimeter (Mettler-Toledo,

Table 1

Polyphenol (PP) content, diglyceride ratio (1,2 DAGs / 1,3 DAGs), tocopherols, absorbance at 232 (K232) and 270 nm (K270), peroxide value (PV), acidity index, and viscosity of the control oil (High-P), the oil-containing intermediate polyphenol content (Medium-P) and the polyphenol removed oil (No-P).

Oil Sample	PP Content (mg/kg)	1,2/1,3 DAGs	Tocopherols (mg/kg)	K_{232}	K_{270}	PV (mEq O_2/kg)	Acidity	Viscosity (mPa s)
High-P (control)	322.9 ± 10.7 [a]	1.25 ± 0.00 [a]	354.59 ± 2.13 [a]	2.24 ± 0.08 [a]	0.06 ± 0.01 [a]	7.6 ± 0.1 [b]	0.41 ± 0.01 [a]	77 ± 1 [a]
Medium-P	173.0 ± 9.3 [b]	1.31 ± 0.26 [a]	340.87 ± 2.31 [b]	2.13 ± 0.11 [ab]	0.04 ± 0.01 [a]	8.9 ± 0.1 [a]	0.32 ± 0.01 [b]	78 ± 2 [a]
No-P	n.d.	1.39 ± 0.03 [b]	340.80 ± 3.26 [b]	1.84 ± 0.06 [b]	0.06 ± 0.01 [a]	9.1 ± 0.2 [a]	0.24 ± 0.02 [c]	74 ± 3 [a]

n.d. not detectable.

Lowercase superscript letters (a–c) indicate significant differences among the different oils (P < 0.05).

Greifensee, Swiss) connected to a GraphWare software TAT72.2/5 (Mettler-Toledo) was used for DSC analysis. Heat flow calibration was achieved using indium (heat of fusion 28.45 J g^{-1}). Temperature calibration was carried out using hexane (m.p. − 93.5 °C), water (m.p. 0.0 °C), and indium (m.p. 156.6 °C). Aliquots of 60–80 mg oleogels were weighed in 100 µL aluminum DSC pans and heated from 20 to 100 °C at 5 °C min^{-1} in the DSC cell under nitrogen flow (20 mL min^{-1}) while using an empty pan as a reference. The temperature corresponding to the transition peak (T_{peak}), and the melting enthalpy (ΔH) were computed (STARe, ver.8.10, Mettler-Toledo).

2.4.6. Fourier transform infrared (FT-IR) measurement

Oleogels infrared spectra were recorded using an FT-IR spectrophotometer, equipped with an ATR accessory and a Zn-Se crystal allowing the direct collection of IR spectra on a sample without any preparation (Alpha-P, Bruker Optics, Milan, Italy). A background scan of the clean crystal was acquired before sample scanning. Spectra were collected at 25 ± 1 °C in the range 4000–400 cm^{-1} at a resolution of 4 cm^{-1} and with 32 co-added scans. Data were processed by the OPUS software (version 7.0, Bruker Optics).

2.4.7. Synchrotron X-ray diffraction (XRD) analysis

X-ray diffraction patterns were recorded at the X-ray diffraction beam-line 5.2 at the Synchrotron Radiation Facility Elettra in Trieste (Italy). The X-ray beam emitted by the wiggler source on the Elettra 2 GeV electron storage ring was monochromatized by a Si(1 1 1) double crystal monochromator, foc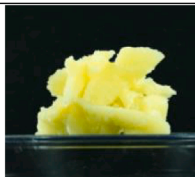used on the sample and collimated by a double set of slits giving a spot size of 0.2 × 0.2 mm. A drop of the sample was lodged into a nylon pre-mounted cryoloop 20 mm for crystallographic experiments (0.7–1.0 mm) (Hampton re- search HR4-965, Aliso Veijo, CA, USA). The sample temperature was controlled by means of a 700 series cryocooler (Oxford Cryosystems,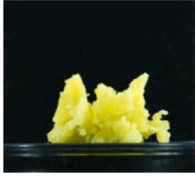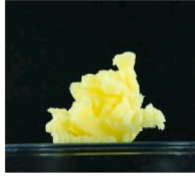 Oxford, UK) with an accuracy of ∼ 1 °C. Analyses were performed at 20 °C. Data were collected at a photon energy of 8.856 keV (l 1⁄4 1.4 Å), using a 2 M Pilatus silicon pixel X-ray detector (DECTRIS ltd., Baden, Switzerland). Bidimensional patterns collected with Pilatus were calibrated by means of a LaB6 standard and integrated using the software FIT2D (Hammersley, 2016). The indexing of the XRD patterns obtained by the crystalline phases was performed using the program Winplotr (Roisnel & Rodríguez-Carvajal, 2001) and Checkcell (Iaugier & Bocu, 2021).
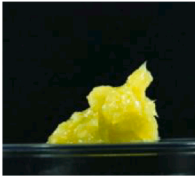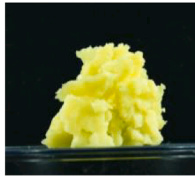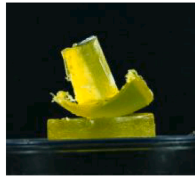
2.5. Statistical analysis

Results are averages of three measurements carried out on two replicated experiments and are reported as means ± standard deviation. Analysis of variance (ANOVA) was performed using R (version 4.0.3, The R Foundation for Statistical Computing, Vienna, Austria). Bartlett's test was used to check the homogeneity of variance and the Tukey test was used to test for differences between means ($p < 0.05$).

Table 2

Macroscopic visual appearance of oleogels prepared with 10% (w/w) of monoglycerides (MG), rice bran wax (RW), sunflower wax (SW), or the mixture of β-sitosterol and γ-oryzanol (PS) in EVOO having decreasing polyphenol content.
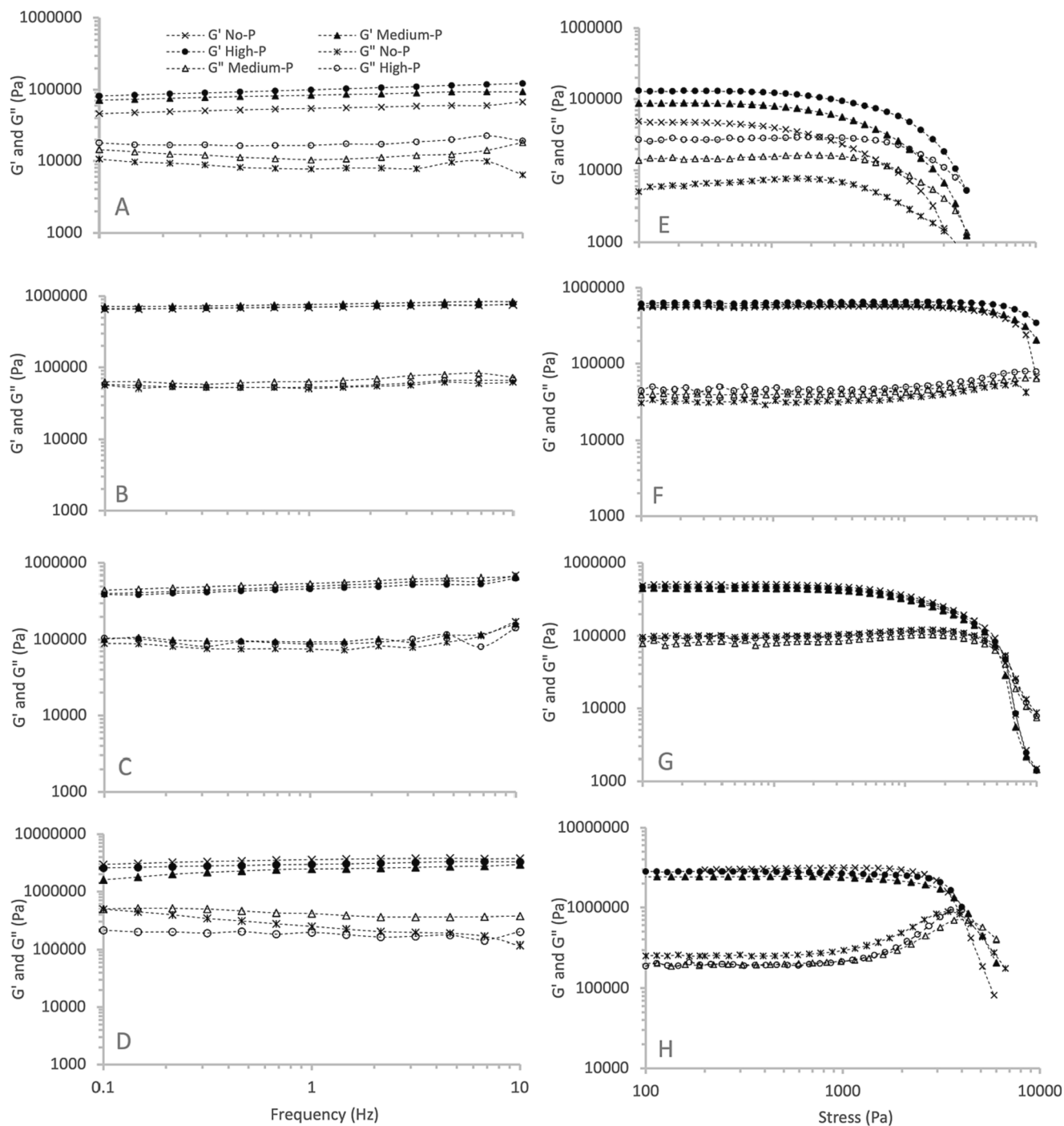
Fig. 1. Frequency and oscillatory stress sweep curve of EVOO oleogels containing 10% (w/w) monoglycerides (A, E), rice bran wax (B, F), sunflower wax (C, G), or a mixture of β-sitosterol and γ-oryzanol (D, H) prepared with EVOO having different polyphenol content.

3. Results and discussion

3.1. Chemical characterization

Table 1 shows the chemical characteristics of the EVOO samples having different polyphenol content. It can be noted that the procedure applied to remove polyphenols from EVOO was effective, as no polyphenols were detected in the No-P sample. The other two oils presented 322.9 mg kg^{-1} (High-P) and 173.0 mg kg^{-1} (Medium-P) as polyphenol content. The procedure applied to remove polyphenols allowed to maintain all EVOO quality parameters in a range complying with the compulsory limits reported in the REG CEE n.2568/91. In particular, no

oxidation phenomena were triggered since neither the peroxide value, nor the K$_{232}$ and K$_{270}$, revealing the formation of conjugated dienes and trienes. Moreover, the method applied did not affect the fatty acid profile (Table S1). Lastly, no more than 5% polyphenol depletion was detected for all gelators (data not shown).

Additionally, it should be noted that no polarity changes are not expected upon polyphenol removal. In fact, the dielectric constant of EVOO reported in the literature is comparable to that of vegetable oils undergoing the refining process (Lizhi, Toyoda, & Ihara, 2008).

Table 3
Rheological parameters (G′, G″, Tan δ at 1 Hz, and critical stress) of oleogels containing 10% (w/w) monoglycerides (MG), rice bran wax (RW), sunflower wax (SW), and a mixture of β-sitosterol and γ-oryzanol (PS) prepared with No-P, Medium-P, and High-P oils.

Oleogelator	Sample	G′ x 10^4 (Pa)	G″ x 10^4 (Pa)	Tan δ	Critical stress (Pa)
MG	High-P (control)	9.3 ± 1.0 [a]	1.5 ± 0.2 [a]	0.165 ± 0.012 [a]	12.32 ± 1.16 [a]
	Medium-P	8.2 ± 1.7 [a]	1.3 ± 0.4 [ab]	0.155 ± 0.003 [a]	12.29 ± 2.95 [a]
	No-P	6.2 ± 0.7 [b]	0.8 ± 0.1 [b]	0.130 ± 0.010 [b]	7.61 ± 1.37 [b]
RW	High-P (control)	68.1 ± 4.3 [a]	5.0 ± 0.2 [a]	0.076 ± 0.002 [a]	464.95 ± 7.06 [a]
	Medium-P	68.1 ± 6.7 [a]	5.5 ± 0.5 [a]	0.079 ± 0.002 [a]	317.56 ± 3.52 [b]
	No-P	68.7 ± 9.9 [a]	5.4 ± 0.5 [a]	0.074 ± 0.004 [a]	287.10 ± 17.60 [c]
SW	High-P (control)	57.1 ± 9.7 [a]	9.1 ± 1.6 [a]	0.164 ± 0.002 [a]	39.18 ± 3.74 [a]
	Medium-P	45.7 ± 8.1 [a]	7.7 ± 1.7 [a]	0.169 ± 0.010 [a]	41.05 ± 4.31 [a]
	No-P	50.5 ± 0.2 [a]	8.6 ± 0.8 [a]	0.171 ± 0.018 [a]	39.87 ± 4.17 [a]
PS	High-P (control)	239.9 ± 2.2 [a]	20.9 ± 3.6 [a]	0.084 ± 0.006 [a]	1966.5 ± 364.8 [a]
	Medium-P	216.0 ± 9.1 [a]	17.8 ± 2.6 [a]	0.082 ± 0.008 [a]	1745.5 ± 202.9 [a]
	No-P	255.0 ± 12.2 [a]	23.7 ± 1.1 [a]	0.087 ± 0.009 [a]	1999.5 ± 388.6 [a]

Superscript letters (a–c) indicate significant differences among oils with different polyphenol content containing the same gelator ($p < 0.05$).

3.2. Oleogel properties

The visual appearance of the EVOO oleogels prepared by using the three different oils and the selected gelators is reported in Table 2. EVOOs were successfully structured into solid-like materials with self-standing behavior and a visual appearance differing depending on the gelator considered. MG and wax-based oleogels were opaque systems; whereas PS showed a translucent appearance, in agreement with the literature (Alongi et al., 2022). No visual differences can be appreciated as a function of oil polyphenol content. All the samples showed an oil binding capacity higher than 99% with no oil release upon centrifugation (data not shown).

To obtain information on oleogel microstructure, viscoelastic properties in both linear (small strain) and non-linear (large strain) regimes were investigated. Fig. 1 shows the rheological behavior of the samples; whereas Table 3 the relevant G′ and G″ at 1 Hz, the tan δ and the critical stress.

Fig. 1 A-D reports the results of the frequency sweep test performed in LVR. As expected for gels, G′ exceeded G″ for all the frequency ranges indicating that the elastic component is dominant. Additionally, a weak dependence of moduli on frequency was observed, which is characteristic of viscoelastic solids. Rheological parameters at a frequency of 1 Hz were used to compare the samples (Table 3). For RW, SW, and PS oleogels, no significant differences in linear viscoelastic parameters were observed between samples with and without polyphenols (p greater than 0.05). In contrast, MG-containing polyphenols exhibited higher G′ and tan δ at 1 Hz compared to the oleogel obtained from EVOO cleared from polyphenols. These results indicate that the matrix of MG structured with High-P oil has more elastic interactions in the crystalline network. It can be inferred that polyphenols can interact with the crystal network reinforcing it by forming additional junction points. The MG-

oleogel obtained from the High-P also presented a slightly greater degree of viscous behavior compared to the sample with No-P, suggesting that the weak interactions promoted by polyphenols were broken down when shear stress was applied to the material, producing an increase in energy dissipation (viscous character) due to the presence of slippery layers.

Oleogelator type influenced the rheological behavior according to a previous investigation (Fayaz, Calligaris, & Nicoli, 2020). PS gave the highest and MG the lowest elastic modulus among gelators attributed to differences in oleogel microstructure (Table 2). The former made the strongest gels mainly due to the ability of self-aggregation of PS tubular elements, promoting the formation of a three-dimensional network (Calligaris et al., 2014).

Fig. 1 E-H shows the results of the oscillatory stress sweep test at 1 Hz, which are useful to determine the limit of the LVR. In the linear region, both viscoelastic moduli are not stress-dependent (*plateau*) because the applied stresses produce a proportional strain response (reversible deformation). The upper limit of LVR was 7.6–12 Pa for MG, 93–124 Pa for RW, 39–41 Pa for SW, and 880–990 Pa for PS oleogels. The critical stress (σ_c) corresponding to the shear stress above which structure breaking occurs, was obtained from G' profile (Fig. 1 E-H). The upper limit of LVR and σ_c was identical for MG and SW oleogels because they both resulted from G' curve. In contrast, the limit of LVR was lower than σ_c for RW and PS samples since the former was evaluated using the G″ profile (narrower *plateau* than G'). Above the σ_c value, the matrix is subjected to permanent deformation due to the breaking up of the inner structure (Patel, Babaahmadi, Lesaffer, & Dewettinck, 2015). The σ_c parameter, which reflects the resistance of the gel network to shear stresses, decreased in the following order: PS > RW > SW > MG (Table 3).

Comparing samples with crystalline network, SW gave σ_c values much lower than RW revealing differences in the intensity of interactions in their networks. Similar evidence was previously reported for these waxes added to medium-chain triacylglycerols (Fayaz, Polenghi, Giardina, Cerne, & Calligaris, 2021). Based on these results, SW samples were weaker than RW. Generally, the number and intensity of interactions influence network strength. Probably, differences in σ_c values between waxes are mainly due to the intensity of interactions since the samples differed slightly in the number of elastic interactions (frequency sweep results, Table 3). These differences were attributed to the chemical compositions of waxes. As reported by Doan et al. (2017), the ester fraction in the waxes represents about 93–96% of the total components. However, this fraction is characterized by a different composition of fatty acids. As can be noted in Table S1, RW was characterized by a prevalence of esters containing oleic acid C18:1, whereas SW showed a higher variability of fatty acids in the ester fraction with C18:1, C18:2, and C20:0 fatty acids as main components. The different wax composition is expected to produce a different ester arrangement, with crystals characterized by a less ordered structure with a lower number of elastic interactions in the case of SW. These crystals are expected to be more susceptible to mechanical stresses compared to those obtained from the tighter and more ordered packing of RW esters (Doan et al., 2017). Similar findings were actually reported in the literature showing that the crystalline network of SW breaks down more easily at the same applied force in comparison with RW (Fayaz et al., 2020; Patel et al., 2015).

The concentration of polyphenols affected the features of oleogels to different extents depending on the network. PS- and SW-based oleogels did not show significant changes in the critical stress between samples with and without polyphenols (Table 3). On the contrary, the magnitude of σ_c was significantly higher for MG and RW samples containing polyphenols, indicating a structuring effect ($p < 0.05$), that can be attributed once again to the formation of junction points in the crystalline network through polyphenols. For RW, σ_c increased also with polyphenol content, resulting in 11–62% higher compared to No-P.

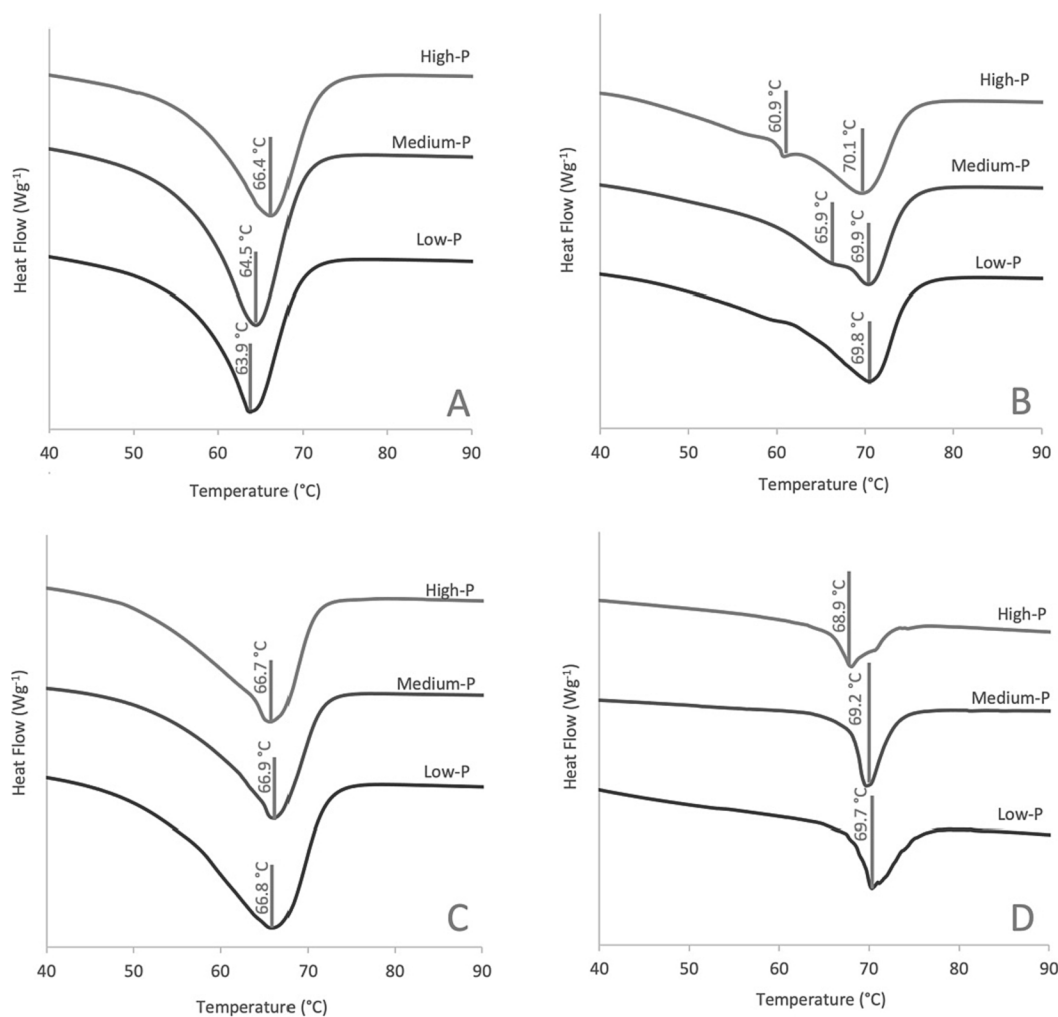Looking at the non-linear regime (Fig. 1 E-H), both G' and G″

Fig. 2. Melting calorimetric curves of oleogels containing 10% (w/w) monoglycerides (A), rice bran wax (B), sunflower wax (C), and a mixture of *β*-sitosterol and *γ*-oryzanol (D) prepared with No-P, Medium-P and High-P oils.

decreased as stress amplitude increased for MG-based oleogels due to network breakage. For PS samples, G″ showed an increase followed by a decrease as stress (or strain) rose revealing a weak strain overshoot behavior (Hyun, Kim, Ahn, & Lee, 2002). Therefore, a characteristic of the PS network is to resist deformation (increase in G″) before breaking.

Based on G' and tan δ at 1 Hz from frequency sweep (LVR) and σ_c values (Tavernier et al., 2017), MG and SW gave the weakest and PS the strongest oleogels (Table 3).

The impact of polyphenols was then studied with calorimetric analysis. Fig. 2 shows the melting curve of the samples. All oleogels revealed broader endothermic peaks with lower T_{peak} in comparison to the neat gelators (Fig. S1). This result is expected and in agreement with the literature and is associated with the initial disintegration of the network in oil followed by the melting of crystals in MG, SW, and RW-based oleogels or the de-structuring of the tubules in the PS-containing sample (Alongi et al., 2022). Considering the effect of polyphenol content, MG-oleogels presented a progressive decrease of the T_{peak} as the polyphenol content also decreased, indicating a reduction in the network's strength as polyphenols in the matrix decreased. It can be hypothesized that the absence of polyphenols reduced the number of junction points able to stabilize the network, making the latter more susceptible to melting at lower temperatures. Moving to RW-containing samples, two melting events can be noted in the High-P sample (T_{peak}' at 60 °C e T_{peak}'' at 70 °C). These can be associated with the crystallization of two fractions, as also noted in the neat gelator (Fig. S1). Interestingly, the peak at the lowest temperature disappeared as the polyphenol in the

matrix decreased, confirming that polyphenols may play a critical role in stabilizing the crystalline RW network, ultimately affecting oleogel behavior.

The differences in the oleogel properties previously described can be associated with the microscopic features of the network. Thus, polarized light microscopy was performed on samples containing crystals (MG, RW, and SW). It should be remembered that, as well known in the literature, it is not possible to image the network formed by the mixture of phytosterol with sterol-esters because they form tubules with dimensions that are considerably smaller than the wavelength of visible light (Bot et al., 2008; Calligaris et al., 2014).

The crystalline networks formed by MG, RW, and SW are well appreciable in the microscopy images reported in Table 4 in which bright areas are the crystals and the dark zones that fill the space correspond to the liquid oil.

The MG in the control EVOO formed a network made of randomly dispersed needle-like crystals. As reported in the literature, MG organized itself into an inverse lamellar phase with a *β*-subcell packing in oil (da Pieve et al., 2010). Considering waxes, SW showed needle-like crystals, whereas RW formed spherulites well dispersed in the matrix. Respectively, these results agree with Doan et al. (2015) and Fayaz et al. (2020) and can be associated with the different chemical compositions of waxes (Table S1) leading to a different crystal morphology.

The progressive lower content of polyphenols in the samples, determined differences in the oleogel network structure, especially in MG- and RW-containing samples, whereas the SW oleogel network

Table 4

Microscopic appearance of oleogels containing 10% (w/w) monoglycerides (MG), rice bran wax (RW), and sunflower wax (SW) prepared with No-P, Medium-P and High-P oils. Magnification: 40x and 400x.

Sample	MG	RW	SW
High-P (Control)			
Medium-P			
No-P			
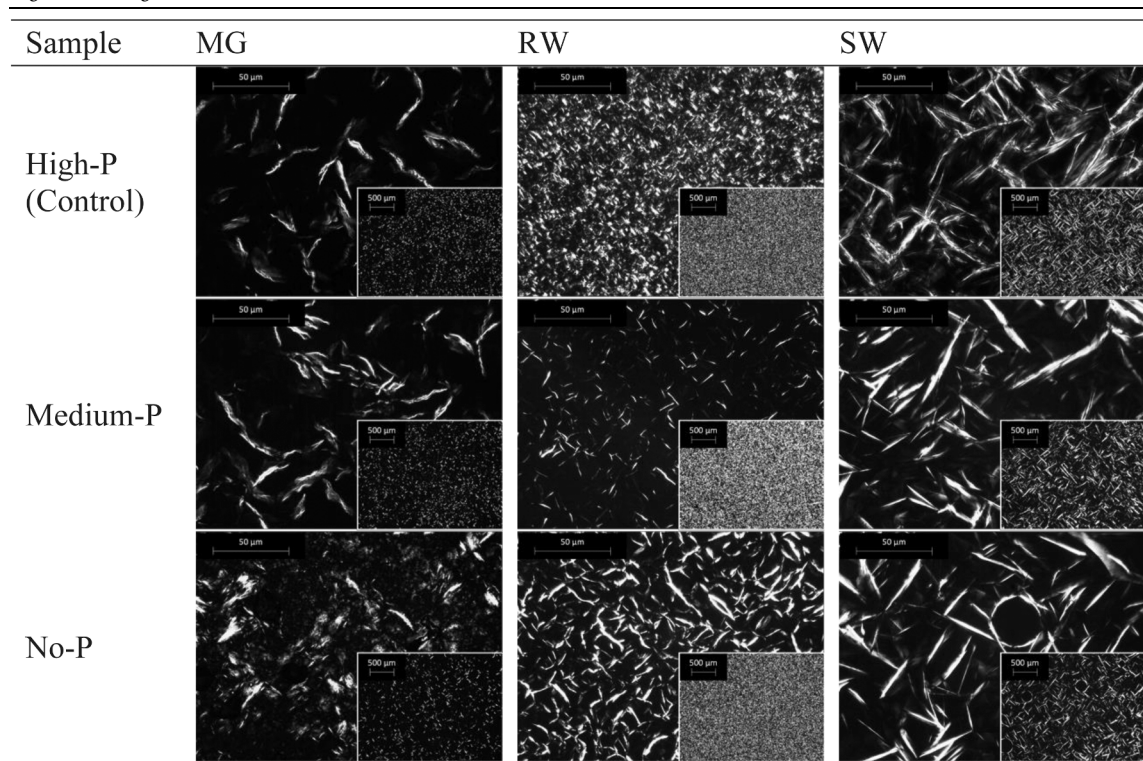
seems to be comparable among No-P, Medium-P, and High-P oils. In MG and RW samples the crystal morphology and density resulted different from the control samples. In the case of RW, the morphology of the crystals appeared to change from spherules to needle-like crystals with a higher dimension. In the MG-oleogel, crystals were more randomly dispersed with fewer connections.

The network structure changes associated with the polyphenol content confirmed the importance of these components in the network formation in MG and RW. It can be inferred that in both cases polyphenols participate in the network strengthening and reinforcing the connections among crystals possibly creating new junction points. As described by other authors, olive polyphenols display surface activity (di Mattia et al., 2014; Giacintucci et al., 2018). Hence, it can be hypothesized that they locate near to polar moieties in MG and RW favoring and increasing the degree of interactions among crystals (Shang, Zhong, Zhu, Huang, & Li, 2021).

The ineffectiveness of polyphenols in reinforcing SW oleogel compared to RW could be attributed to the lower gel strength (Table 3) associated with a different wax composition (Table S1). As previously reported (Fayaz et al., 2020) SW produces dendritic crystals larger than the spherulitic ones obtained from RW, in which the potential contribution of polyphenols to the gel network was probably masked. Finally, the results on PS-based oleogels indicated that polyphenols did not interact with the tubule formation between β-sitosterol and γ-oryzanol, even though other authors evidenced that the micro- and nanostructural properties of the tubular self-assembled system were affected by the presence of phenolic moieties under different gelling conditions, such as gelator concentration and ratios, and cooling rate (Martins, Cerqueira, Vicente, Cunha, Pastrana, & Cerqueira, 2022).

To evaluate the molecular interactions in the samples, FT-IR spectroscopy was performed (Fig. S2). All oleogel spectra presented the typical bands associated with triglycerides, being the major components of EVOO, such as the double peak in 3000–2800 cm^{-1} region (alkane sp^3 C—H stretching vibration of ethyl and methyl groups) and a smaller one

at 1700 cm^{-1} (stretching vibration of carbonyl group C=O) (Singh, Pal, Pradhan, & Pramanik, 2013). The region below 1500 cm^{-1} is commonly called the "fingerprint region" and here most of the differences are due to the intermolecular feature of each compound which is expressed by a complex set of bands.

The FT-IR spectra of samples were different depending on the gelator, however, no differences were detected among samples with different polyphenol content. As reported by Öğütcü and Yilmaz (2014), intermolecular hydrogen bonds should appear as medium-intensity bands in the bands at 3450–3550 cm^{-1} wavenumber range, and intramolecular hydrogen bonds as medium-intensity bands in the 3540–3570 cm^{-1} wavenumber range. Since no signals relevant to hydrogen bonds in the FT-IR spectra were recorded, this means probably that polyphenols did not chemically interact with the gelators, but only Van der Waals interactions occurred.

Finally, to understand the crystal polymorphs formed in the samples, synchrotron XRD analyses were performed (Fig. S3). These patterns are in agreement with data reported in the literature (Fayaz et al., 2017; Li, Guo, Bi, Zhang, & Xu, 2021; Valoppi, Calligaris, Barba, Šegatin, Poklar Ulrih, & Nicoli, 2017). MG showed a multitude of peaks in the WAXD region, attributable to β' polymorphic form crystals. The two waxes presented two peaks in the WAXD region along with the previously observed and oil-related SAXD peaks. WAXD peaks appeared to be very similar not only inside the same gelator group but also between the two different waxes and this can be explained by the same form β' polymorphic form (Valoppi et al., 2017). Different levels of polyphenols do not contribute to crystal conformation in all samples, which is highlighted by the absence of peak deviations detected between the three different oils used in oleogel preparation.

Based on these results, it can be inferred that polyphenols were able to generate additional interactions among crystals in MG and RW modifying the microstructural organization of the networks and thus the macrostructure. On the contrary, at the nano-level crystals maintained their original morphology.

4. Conclusions

Results acquired in this study clearly evidenced that polyphenols could differently impact the structure of oleogels. While no networking capacity was noted in phytosterol-based oleogels, EVOO polyphenols were able to reinforce the interactions among crystals in MG- and RW-containing samples probably forming additional junction points in the network through Van der Waals forces. Despite the crystallinity of the SW-oleogel network, its structure was not affected by the presence of polyphenols. It is likely that polyphenols need to encounter a significant number of polar groups to induce a network structure modification. Overall, this study confirmed the strong importance of minor components in vegetable oils in affecting the micro- and macro-structure of oleogels. Based on these results, further investigation is necessary to better understand how polyphenol participation in the oleogel network could affect their stability against oxidative reactions as well as their biological fate in the human body. It is also not excluded the possibility to intentionally use polyphenols as innovative structuring agents with the dual role of bioactive molecules and techno-functional ingredients.

CRediT authorship contribution statement

Francesco Ciuffarin: Investigation, Data curation, Visualization, Writing – original draft. **Marilisa Alongi:** Methodology, Data curation, Visualization, Writing – review & editing. **Donatella Peressini:** Methodology, Writing – review & editing. **Luisa Barba:** Methodology, Investigation, Writing – review & editing. **Paolo Lucci:** Methodology, Writing – review & editing, Validation. **Sonia Calligaris:** Conceptualization, Writing – original draft, Resources, Supervision.

Declaration of Competing Interest

The authors declare that they have no known competing financial interests or personal relationships that could have appeared to influence the work reported in this paper.

Data availability

Data will be made available on request.

Appendix A. Supplementary data

Supplementary data to this article can be found online at https://doi.org/10.1016/j.foodchem.2023.135572.

References

Alongi, M., Lucci, P., Clodoveo, M. L., Schena, F. P., & Calligaris, S. (2022). Oleogelation of extra virgin olive oil by different oleogelators affects the physical properties and the stability of bioactive compounds. *Food Chemistry, 368*, Article 130779. https://doi.org/10.1016/j.foodchem.2021.130779

Bot, A., den Adel, R., & Roijers, E. C. (2008). Fibrils of γ-oryzanol + β-sitosterol in edible oil organogels. *JAOCS, Journal of the American Oil Chemists' Society, 85*(12), 1127–1134. https://doi.org/10.1007/s11746-008-1298-7

Calligaris, S., Alongi, M., Lucci, P., & Anese, M. (2020). Effect of different oleogelators on lipolysis and curcuminoid bioaccessibility upon in vitro digestion of sunflower oil oleogels. *Food Chemistry, 314*, 126–146. https://doi.org/10.1016/j.foodchem.2019.126146

Calligaris, S., Mirolo, G., da Pieve, S., Arrighetti, G., & Nicoli, M. C. (2014). Effect of Oil Type on Formation, Structure and Thermal Properties of γ-oryzanol and β-sitosterol-Based Organogels. *Food Biophysics, 9*(1), 69–75. https://doi.org/10.1007/s11483-013-9318-z

Co, E. D., & Marangoni, A. G. (2012). Organogels: An alternative edible oil-structuring method. In *JAOCS. Journal of the American Oil Chemists' Society, 89*(5), 749–780. https://doi.org/10.1007/s11746-012-2049-3

da Pieve, S., Calligaris, S., Co, E., Nicoli, M. C., & Marangoni, A. G. (2010). Shear Nanostructuring of monoglyceride organogels. *Food Biophysics, 5*(3), 211–217. https://doi.org/10.1007/s11483-010-9162-3

di Mattia, C., Paradiso, V. M., Andrich, L., Giarnetti, M., Caponio, F., & Pittia, P. (2014). Effect of olive oil phenolic compounds and maltodextrins on the physical properties and oxidative stability of olive oil O/W emulsions. *Food Biophysics, 9*(4), 396–405. https://doi.org/10.1007/s11483-014-9373-0

Doan, C. D., To, C. M., de Vrieze, M., Lynen, F., Danthine, S., Brown, A., … Patel, A. R. (2017). Chemical profiling of the major components in natural oil to elucidate their role in liquid oil structuring. *Food Chemistry, 214*, 717–725. https://doi.org/10.1016/j.foodchem.2016.07.123

Doan, C. D., van de Walle, D., Dewettinck, K., & Patel, A. R. (2015). Evaluating the oil-gelling properties of natural waxes in rice bran oil: Rheological, thermal, and microstructural study. *JAOCS, Journal of the American Oil Chemists' Society, 92*(6), 801–811. https://doi.org/10.1007/s11746-015-2645-0

European Commission. (2020). Farm to Fork Strategy. In *DG SANTE/Unit 'Food information and composition, Food waste'*. https://ec.europa.eu/food/sites/food/files/safety/docs/f2f_action-plan_2020_strategy-info_en.pdf.

Fayaz, G., Calligaris, S., & Nicoli, M. C. (2020). Comparative Study on the Ability of Different Oleogelators to Structure Sunflower Oil. *Food Biophysics, 15*(1), 42–49. https://doi.org/10.1007/s11483-019-09597-9

Fayaz, G., Goli, S. A. H., Kadivar, M., Valoppi, F., Barba, L., Calligaris, S., & Nicoli, M. C. (2017). Potential application of pomegranate seed oil oleogels based on monoglycerides, beeswax and propolis wax as partial substitutes of palm oil in functional chocolate spread. *LWT, 86*, 523–529. https://doi.org/10.1016/j.lwt.2017.08.036

Fayaz, G., Polenghi, O., Giardina, A., Cerne, V., & Calligaris, S. (2021). Structural and rheological properties of medium-chain triacylglyceride oleogels. *International Journal of Food Science and Technology, 56*(2), 1040–1047. https://doi.org/10.1111/ijfs.14757

Giacintucci, V., Di Mattia, C. D., Sacchetti, G., Flamminii, F., Gravelle, A. J., Baylis, B., … Pittia, P. (2018). Ethylcellulose oleogels with extra virgin olive oil: The role of oil minor components on microstructure and mechanical strength. *Food Hydrocolloids, 84*, 508–514. https://doi.org/10.1016/j.foodhyd.2018.05.030

Hammersley, A. P. (2016). FIT2D: A multi-purpose data reduction, analysis and visualization program. *Journal of Applied Crystallography, 49*, 646–652. https://doi.org/10.1107/S1600576716000455

Hooper, L., Martin, N., Jimoh, O. F., Kirk, C., Foster, E., & Abdelhamid, A. S. (2020). Reduction in saturated fat intake for cardiovascular disease. *Cochrane Database of Systematic Reviews, 2020*(8), Article 011737. https://doi.org/10.1002/14651858.CD011737.pub3

Hyun, K., Kim, S. H., Ahn, K. H., & Lee, S. J. (2002). Large amplitude oscillatory shear as a way to classify the complex fluids. *Journal of Non-Newtonian Fluid Mechanics, 107*(1–3), 51–65. https://doi.org/10.1016/S0377-0257(02)00141-6

Iaugier, J., & Bocu, B. (n.d.). Suite of Programs for the interpretation of X-ray Experiments. In *ACM SIGPLAN Notices* (Vol. 49, Issue 10). ENSP/Laboratorie des Matèriaux et du Gènie Physique, BP 46. Retrieved September 13, 2021, from https://www.grenoble-inp.fr/LMGP.

Li, J., Guo, R., Bi, Y., Zhang, H., & Xu, X. (2021). Comprehensive evaluation of saturated monoglycerides for the forming of oleogels. *LWT, 151*, Article 112061. https://doi.org/10.1016/j.lwt.2021.112061

Lizhi, H., Toyoda, K., & Ihara, I. (2008). Dielectric properties of edible oils and fatty acids as a function of frequency, temperature, moisture and composition. *Journal of Food Engineering, 88*(2), 151–158. https://doi.org/10.1016/j.jfoodeng.2007.12.035

Lucci, P., Bertoz, V., Pacetti, D., Moret, S., & Conte, L. (2020). Effect of the refining process on total hydroxytyrosol, tyrosol, and tocopherol contents of olive oil. *Foods, 9*(3), Article 9030292. https://doi.org/10.3390/foods9030292.

Marangoni, A. G., & Garti, N. (2018). Edible Oleogels. In *Edible Oleogels*. Elsevier. https://doi.org/10.1016/c2017-0-00541-4.

Martín-Peláez, S., Castañer, O., Konstantinidou, V., Subirana, I., Muñoz-Aguayo, D., Blanchart, G., … Fitó, M. (2017). Effect of olive oil phenolic compounds on the expression of blood pressure-related genes in healthy individuals. *European Journal of Nutrition, 56*(2), 663–670. https://doi.org/10.1007/s00394-015-1110-z

Martins, A. J., Cerqueira, F., Vicente, A. A., Cunha, R. L., Pastrana, L. M., & Cerqueira, M. A. (2022). Gelation Behavior and Stability of Multicomponent Sterol-Based Oleogels. Gels, 8(1), Article 8010037. https://doi.org/10.3390/gels8010037.

Martins, A. J., Vicente, A. A., Cunha, R. L., & Cerqueira, M. A. (2018). Edible oleogels: An opportunity for fat replacement in foods. *Food and Function, 9*(2), 758–773. https://doi.org/10.1039/C7FO01641g

Öğütcü, M., & Yilmaz, E. (2014). Oleogels of virgin olive oil with carnauba wax and monoglyceride as spreadable products. *Grasas y Aceites, 65*(3), Article 0349141. https://doi.org/10.3989/gya.0349141.

Owen, R. W., Giacosa, A., Hull, W. E., Haubner, R., Spiegelhalder, B., & Bartsch, H. (2000). The antioxidant/anticancer potential of phenolic compounds isolated from olive oil. *European Journal of Cancer, 36*(10), 1235–1247. https://doi.org/10.1016/S0959-8049(00)00103-9

Patel, A. R. (2020). Biopolymer-based oleocolloids. In K. Pal, I. Banerjee, P. Sarkar, D. Kim, W.-.-P. Deng, N. K. Dubey, & K. Majumder (Eds.), *Biopolymer-Based Formulations: Biomedical and Food Applications* (pp. 587–604). Elsevier. https://doi.org/10.1016/B978-0-12-816897-4.00024-2.

Patel, A. R., Babaahmadi, M., Lesaffer, A., & Dewettinck, K. (2015). Rheological Profiling of Organogels Prepared at Critical Gelling Concentrations of Natural Waxes in a Triacylglycerol Solvent. *Journal of Agricultural and Food Chemistry, 63*(19), 4862–4869. https://doi.org/10.1021/acs.jafc.5b01548

Patel, A. R., & Dewettinck, K. (2016). Edible oil structuring: An overview and recent updates. *Food and Function, 7*(1), 20–29. https://doi.org/10.1039/c5fo01006c

Roisnel, T., & Rodríguez-Carvajal, J. (2001). WinPLOTR: A windows tool for powder diffraction pattern analysis. *Materials Science Forum, 378–381*(I), 118–123. https://doi.org/10.4028/www.scientific.net/msf.378-381.118

Rovellini, P. (2017). Oli, grassi animali e vegetali e loro sottoprodotti, semi e frutti oleaginosi". Progetto UNI1603053 Determinazione del Contenuto di Idrossitirosolo e Tirosolo Negli Oli di Olive—Metodo HPLC. *UNI/CT, 003/GL,* 18.

Shang, J., Zhong, F., Zhu, S., Huang, D., & Li, Y. (2021). Formation, structural characteristics and physicochemical properties of beeswax oleogels prepared with tea polyphenol loaded gelators. *Food & Function, 12*(4), 1662–1671. https://doi.org/10.1039/D0FO02772C

Singh, V. K., Pal, K., Pradhan, D. K., & Pramanik, K. (2013). Castor oil and sorbitan monopalmitate based organogel as a probable matrix for controlled drug delivery. *Journal of Applied Polymer Science, 130*(3), 1503–1515. https://doi.org/10.1002/app.39315

Tavernier, I., Doan, C. D., van de Walle, D., Danthine, S., Rimaux, T., & Dewettinck, K. (2017). Sequential crystallization of high and low melting waxes to improve oil structuring in wax-based oleogels. *RSC Advances, 7*(20), 12113–12125. https://doi.org/10.1039/c6ra27650d

Valoppi, F., Calligaris, S., Barba, L., Šegatin, N., Poklar Ulrih, N., & Nicoli, M. C. (2017). Influence of oil type on formation, structure, thermal, and physical properties of monoglyceride-based organogel. *European Journal of Lipid Science and Technology, 119*(2), Article 20150054. https://doi.org/10.1002/ejlt.201500549.

Valoppi, F., Calligaris, S., & Marangoni, A. G. (2017). Structure and physical properties of oleogels containing peanut oil and saturated fatty alcohols. *European Journal of Lipid Science and Technology, 119*(5), Article 201600252. https://doi.org/10.1002/ejlt.201600252.

Vijay, V., Pimm, S. L., Jenkins, C. N., & Smith, S. J. (2016). The impacts of oil palm on recent deforestation and biodiversity loss. *PLoS ONE, 11*(7), Article 0159668. https://doi.org/10.1371/journal.pone.0159668.

Wijarnprecha, K., Aryusuk, K., Santiwattana, P., Sonwai, S., & Rousseau, D. (2018). Structure and rheology of oleogels made from rice bran wax and rice bran oil. *Food Research International, 112*(2018), 199–298. https://doi.org/10.1016/j.foodres.2018.06.005

Yilmaz, E., & Ölütcü, M. (2015). The texture, sensory properties and stability of cookies prepared with wax oleogels. *Food and Function, 6*(4), 1194–1204. https://doi.org/10.1039/c5fo00019j